



HAL
open science

OH kinetics in photo-triggered discharges used for VOCs conversion

L. Magne, N. Blin-Simiand, K. Gadonna, P. Jeanney, F. Jorand, S. Pasquiers,
C. Postel

► **To cite this version:**

L. Magne, N. Blin-Simiand, K. Gadonna, P. Jeanney, F. Jorand, et al.. OH kinetics in photo-triggered discharges used for VOCs conversion. *European Physical Journal: Applied Physics*, 2009, 47 (2), pp.1-9. 10.1051/epjap/2009093 . hal-00486865

HAL Id: hal-00486865

<https://hal.science/hal-00486865>

Submitted on 27 May 2010

HAL is a multi-disciplinary open access archive for the deposit and dissemination of scientific research documents, whether they are published or not. The documents may come from teaching and research institutions in France or abroad, or from public or private research centers.

L'archive ouverte pluridisciplinaire **HAL**, est destinée au dépôt et à la diffusion de documents scientifiques de niveau recherche, publiés ou non, émanant des établissements d'enseignement et de recherche français ou étrangers, des laboratoires publics ou privés.

OH KINETICS IN PHOTO-TRIGGERED DISCHARGES USED FOR VOCs CONVERSION

L. Magne^a, N. Blin-Simiand, K. Gadonna, P. Jeanney, F. Jorand, S. Pasquiers^a, and C. Postel

Laboratoire de Physique des Gaz et des Plasmas - CNRS (UMR 8578)
Université Paris-Sud, Bât.210, 91405 Orsay cedex, France

^a e-mail : lionel.magne@u-psud.fr, stephane.pasquiers@u-psud.fr

Abstract

The kinetic of the hydroxyl radical is studied in $N_2/O_2/H_2O$ mixtures with small amounts of acetone or isopropyl alcohol (0.5 %). The radical density is measured in absolute value in the afterglow of a photo-triggered discharge, which generates an homogeneous transient non-equilibrium plasma, using a time resolved absorption measurement method. For dry mixtures, experimental results are compared to predictions of a self-consistent 0D discharge and kinetic model. It is shown that dissociation of the VOCs through quenching collisions of nitrogen metastable states plays an important role in the production of OH. Measurements can not be explained looking only at the oxidation of acetone or IPA by the oxygen atom. This result is reinforced by experimental results about the OH density in wet mixtures, with or without VOCs, compared to dry ones.

PACS: Plasma high-pressure 52.77.Fv
Plasma reactions 82.33.Xj
Plasma diagnostics 52.70.-m

1. Introduction

Abatement of Volatile Organic Compounds (VOCs) using non-thermal plasmas is attracting many interests [1-4]. For various VOCs, the OH radical is known to be one of the most important reactive species involved in the removal of the pollutant molecule. This radical is efficiently produced during the discharge by dissociative electron collisions on H₂O or reaction of the water molecule with the first excited state of the oxygen atom. Thereafter OH reacts with the VOC. For dry mixtures, O is usually assumed to be the most important species for the conversion of the pollutant. However the hydroxyl radical, which is much more reactive with numerous VOCs than the oxygen atom at a temperature close to the ambient one, can be produced through numerous kinetic processes. In particular, it was recently demonstrated by works on homogeneous discharges [5] that the recombination of O- and H-atoms, through three body collisions involving background molecules, is an efficient OH production process in high pressure and low temperature non-thermal plasmas. Therefore the relative importance of O and OH for the removal of VOCs by pulsed discharges deserves to be studied in more details.

Numerous works have been devoted to the use of dielectric barrier (DBD) or corona discharges for the de-VOC process [1-4]. However such discharges are characterised by highly non-homogeneous transient plasmas for which diagnostics of primary radicals and developments of self-consistent modelling are very difficult. Reduced kinetic schemes should be used in physical and chemical multi-dimensional modelling of the streamer micro-discharge in order to avoid numerical problems as well as prohibitive computer times. However such schemes (set of reactions, type of by-products and rate constants) must be previously validated in such a way that some physical hypothesis about the electrical energy deposition in the pulsed discharge, in time and in space, do not interfere with the understanding of the chemical activity of the energised gas mixture.

We use an homogeneous pre-ionised (photo-triggered) discharge [6] in order to avoid problems in connection with density and temperature gradients. The photo-triggering technique allows to achieve homogeneous transient high-pressure plasmas in various types of gas mixtures, in particular those with atmospheric gases N₂, O₂, and H₂O [7, 8]. Therefore measurements are compared to predictions of a self-consistent 0D discharge and kinetic model which takes into account all relevant reactions for OH and the VOC molecule. Isopropyl alcohol (IPA) is chosen as a test molecule for the present study. Acetone has been found to be the main by-product of IPA conversion by photo-triggered discharges or DBDs

[9-11], so that the role of OH on acetone abatement is also under investigation. The removal of acetone and IPA in air at atmospheric pressure has been already studied by numerous authors since the middle of the nineties, either using non-homogeneous pulsed discharges [12-18] (DBDs, coronas, surface discharges) or coupling such discharges with catalysts [19-25]. However a detailed and experimentally validated plasma kinetic scheme has not been yet proposed. Our objective is to achieve a comprehensive understanding of the hydroxyl radical kinetic in $N_2/O_2/H_2O$ mixtures containing trace of acetone or IPA (concentration less than 1 %). Amongst the various chemical species, radicals and molecules, created by non-equilibrium discharges in such gas mixtures, OH is a good candidate for the validation of kinetic schemes owing to its high reactivity.

The present paper deals with experimental results about the time evolution of the OH density measured in absolute value in the afterglow of a photo-triggered discharge in N_2/O_2 /acetone and N_2/O_2 /IPA, and about the effect of water molecules added to such mixtures. For the dry ones, measurements are compared to predictions of the self-consistent model taking into account an increasing kinetic complexity, i.e. firstly only oxidation reactions, and secondly addition of possible dissociation processes of the VOC molecules through collisions with electrons and with nitrogen excited states. The theoretical study will be extended to wet mixtures in the future.

2. Experimental set-up

The experimental set-up is given in figure 1. The photo-triggered discharge reactor used for this work was described previously [5]. Two electrodes, 50 cm long with a spacing $d=1$ cm and a flat profile over 1 cm width, are directly connected to an energy storage unit of capacitance $C=17.44$ nF charged up to a voltage V_0 in a few hundred nanoseconds. Once V_0 is reached on the electrodes, the gas breakdown is achieved through photo-ionisation of the gas mixture by UV-photons which are produced by an auxiliary corona discharge located at the bottom of the main discharge.

A gas compressor is used to produce a gas flow through the discharge gap. The discharge frequency, 1.25 Hz, is chosen such that the whole reactor volume, 500 cm^3 , is renewed between two discharges. The volume of the experimental device, 9 l, which corresponds to the total volume of the gas mixture studied, is much higher than the discharge one (50 cm^3) owing to the use of a tank in the loop. The total pressure is 460 mbar for an oxygen percentage ranging from 1 % up to 20 %, and for a VOC concentration of 0.5 %. The water vapour concentration is fixed to about 2.3 %.

The initially applied reduced electric field between the gap, $(E/N)_0$, given by $(E/N)_0 = V_0 / (d \cdot N)$ where N is the total density of the gas mixture, is fixed to 200 Td ($V_0 = 23$ kV). The low discharge circuit inductance, 6.5 nH, allows to obtain a short current pulse duration of 60 ns. The electrical energy transferred to the gas mixture is 92 J.l^{-1} (4.6 J deposited in the plasma volume per current pulse).

The time evolution of OH density is measured in the afterglow by optical absorption spectroscopy around 308 nm. Collimated light of a xenon flash lamp passes through the discharge gap (50 cm of absorption length). The transmitted light is then analysed with a 75 cm focal length spectrometer equipped with an intensified pulsed CCD camera. This set-up allows to obtain the whole absorption spectra of the $\text{OH}(X^2\Pi, v''=0) \rightarrow \text{OH}(A^2\Sigma^+, v'=0)$ band with a temporal resolution of 250 ns and a spectral resolution of 0.03 nm. Examples of absorption spectra are given in figure 2. The whole volume of the experimental device is pumped down to 10^{-4} mbar between each set of measurements.

For dry mixtures, possible effect of residual water vapour traces on the experimental results has been carefully checked through absorption measurements in N_2 or in N_2/O_2 without addition of VOCs. No absorption signal has been detected, showing that the detected signal plotted for example in figure 2 can be unambiguously ascribed to the presence of VOC molecules in the gas mixture, and not to residual water vapour. This has been also checked during our previous experiments on OH detection by LIF (density in relative value), with a much lower detection limit than the absorption technique (several orders of magnitude), in both N_2/VOC and $\text{N}_2/\text{O}_2/\text{VOC}$ (VOC : acetone or IPA) [11, 35]. No LIF signal has been detected in N_2 or in N_2/O_2 plasmas.

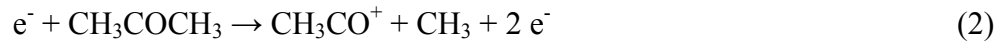
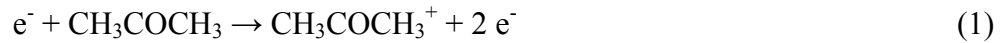
3. Self-consistent modelling

A 0D model has been previously developed [5-8, 26], which couples : i) the solution of the Boltzmann equation for the electrons, ii) the kinetic equations describing the temporal evolution of the various species (molecular excited states, ions, atoms, radicals, molecules) produced during the discharge or during the afterglow, iii) the electric circuit equations given by the Kirchoff laws. Many reaction rates are sensitive functions of the gas temperature so that temperature time evolution is taken into account through the resolution of the energy conservation equation. The Boltzmann equation is solved using algorithms developed by Ségur and Bordage [27]. Details on the code configuration and the numerical procedure are given in [26]. The measured time evolutions of the voltage and the discharge current were

compared to the computed ones in order to check that energy deposition in the plasma composed of atmospheric gases is well predicted by the model [7, 8].

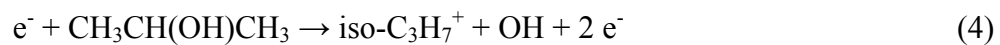
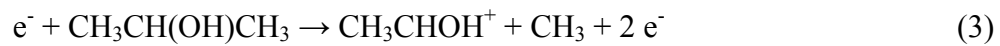
Details about the kinetic scheme adopted for atmospheric gases has been given in [5-8]. As typical examples of model results in the N₂/O₂ mixture, the figure 3 gives the computed time evolutions of excited nitrogen and oxygen molecular species, atoms, and also NO and O₃ for conditions of the experiment and 20 % oxygen in the mixture. Excited species correspond to effective states clustering real molecular levels. The kinetic model includes 43 species which react through 259 processes, including electron collisions on molecules, negative and positive ions reactions (recombination and charge transfers), v-v and v-T processes of N₂, radiative de-excitation and quenchings of excited states, excitation transfers, radical and molecule reactions.

As far as a carbonated molecule is added to N₂/O₂, numerous other kinetic processes are involved in the discharge. As a first step, we have only considered oxidation and dissociation reactions of acetone and IPA, and the kinetics of by-products containing carbon atoms (ions and radicals) have been neglected. Dissociative electron collisions on the VOCs produce neutral and ionic fragments. The most important ionisation processes are, for acetone [28],



The 43 amu fragment ion, CH₃CO⁺, is the major specie for an impact electron energy above 15 eV, and the energy threshold for process (2) is 10.6 eV. However process (1) dominates for an electron energy increasing from the ionisation threshold, 9.7 eV, up to 15 eV [28].

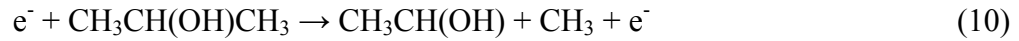
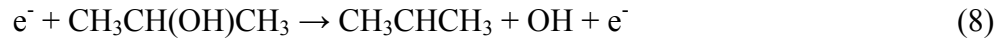
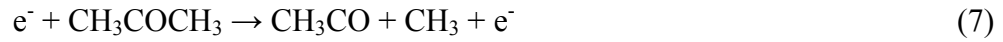
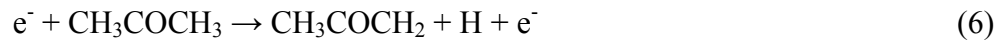
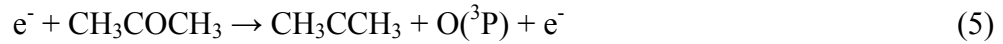
For IPA [29],



process (3) being the dominant one from the ionisation threshold, 10.17 eV, up to at least 90 eV [29].

Reactions (1-4) have been taken into account using collision cross sections given in [28, 29]. Such processes can be a non negligible source of radicals at high values of VOCs concentration in the gas mixture. Nevertheless, in nitrogen based gas mixtures energised by pulsed discharges, dissociation of molecules through ionisation collisions should be less efficient than through excitation of electronic excited states. To the authors knowledge, no data exists (cross section values as well as exit channels) on such processes for acetone and IPA. Therefore we used the known dissociation cross section for propane [30], and we

assumed that H, O(³P), OH, and CH₃ are produced with same probabilities (partial cross sections equal to the overall one multiplied by 0.33), i.e.



with energy thresholds taken equal to corresponding bounding energies.

Of course the oxygen atom in its ground energy level, O(³P), is mainly produced by the dissociative excitation of the oxygen molecule, i.e.



and with same process for other N₂ states, like a¹Σ, a¹Π and w¹Δ. Thereafter acetone and IPA react with O(³P) to produce the hydroxyl radical,



Thereafter OH reacts with VOCs to produce the water molecule and radicals,



Other neutral processes taken into in our model are 86 reactions, added to the ones given above and to the basic set established for N₂/O₂ [5-8], in which the following species are involved : H, O(³P), O(¹D), OH, HO₂, H₂O, H₂O₂, N, NO, NO₂, NO₃, HNO, HNO₂, HNO₃, HNO₄, NH, NH₂, and NH₃.

Coefficients for electron collisions are directly obtained from the solution of the Boltzmann equation, while those for reactions between heavy species (neutrals and ions) have been taken in great part from the NIST database [31] and from a critical review of various compilations [32, 33]. In table 1 are summarised values of rate constants taken into account for neutral reactions cited all through the paper.

Acetone and IPA should also be dissociated through collisions with N₂ metastable states. The rate constant for quenching of the A³Σ_u⁺ state by acetone has been previously measured using a dedicated experiment [34], 1.1×10⁻¹⁰ cm³s⁻¹. However there is no information about by-products. Moreover no data exists for IPA. In a previous study [11, 35], we have estimated

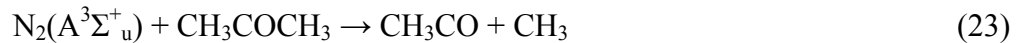
that the rate constants for collision of $A^3\Sigma_u^+$ on acetone and on IPA are about the same, $2.5 \times 10^{-11} \text{ cm}^3\text{s}^{-1}$, but a factor of 4 lower than the value given by Clark and Setser [34] for acetone. It is not yet possible to confirm the exact value for this rate constant. Therefore, in order to emphasise the influence of N_2 states quenching collisions on production of radicals, we have taken the upper value by Clark and Setser for the rate constant of both molecules. We have also assumed the following dissociation routes for IPA,



and same reactions for the singlet states group, $a^1\Sigma$, $a^1\Pi$ and $w^1\Delta$, named $N_2(a')$ in our model. The situation for acetone is a little bit different because only the $N_2(a')$ state has enough energy (8.4 eV) to induce cleavage of the C=O double bond (bonding energy 7.63 eV),



so that we have disregarded other type of collisions, like (22-23) below, for this state. For the $A^3\Sigma_u^+$ state (6.17 eV), productions of H and CH_3 are both energetically allowed (bonding energies respectively equal to 4.23 and 3.62 eV), and therefore we postulate



Production of the hydroxyl radical in N_2 /acetone mixtures was demonstrated by LIF experiments on OH [35], showing that the reaction (21) arises. It is also the case for reaction (20) [11]. However more experiments are needed to determine precisely importance of such processes, as well as reaction (5).

4. Results and discussions for dry mixtures

4.1 Experimental results

In figure 4 is plotted the OH density time evolution measured for dry N_2/O_2 mixtures containing either acetone or IPA; the zero time corresponds to the time of the pre-ionisation pulse. The density profiles have been determined as function of the oxygen percentage in the mixture, between 1 % and 20 %. The maximum radical density, $[OH]_{Max}$, which is governed by the balance between production and loss processes, is achieved at a time of a few microseconds after the discharge current pulse whatever the gas mixture studied. Moreover values of $[OH]_{Max}$ measured for mixtures with either acetone or IPA are very closed, as it can

be seen in figure 5 which shows the maximum density plotted against the oxygen percentage. These results are noteworthy because acetone and IPA have very different rate constants, k_{13} and k_{14} , for reactions with the oxygen atom, (13) and (14), to produce the hydroxyl radical. We have also plotted on this figure the maximum $O(^3P)$ density, $[O(^3P)]_{Max}$, produced in absence of VOC in the mixture. It emphasises that $[OH]_{Max}$ is about 2 % of $[O(^3P)]_{Max}$, except at high O_2 percentage in the mixture. Indeed the maximum hydroxyl radical density saturates as far as the oxygen percentage increases above 10 %. This saturation effect on $[OH]_{Max}$ should be related to an increase of loss processes efficiency.

4.2 Effect of oxidation reactions

The mixture temperature at time values of OH density measurements has been estimated from the self-consistent 0D discharge model; it is around 100°C. It is known that the reaction of $O(^3P)$ and OH with alcohol and ketone depends upon the temperature. With respect to acetone and IPA, only the temperature dependence of k_{14} is not yet known. Without considering a temperature dependence for this rate constant, the ratio k_{14}/k_{13} is 12; on the other hand, using published data for ethanol [31] about the temperature dependence, see table 1, we can estimate a ratio of about 40. Therefore, as the presence of the VOC should have a negligible effect on O-atoms production efficiency for the chosen concentration (0.5 %), the production of OH should be much less efficient in the case of acetone than in the case of IPA if only reactions (13) and (14) are considered. Moreover rate constants for reactions of OH with VOCs, (15-17), are also very different : $k_{15} = 3.6 \times 10^{-13} \text{ cm}^3 \text{ s}^{-1}$ and $k_{16} + k_{17} = 4.4 \times 10^{-12} \text{ cm}^3 \text{ s}^{-1}$ at 100°C, so that $(k_{16} + k_{17})/k_{15} = 12$. As a result the similar time values measured for the OH density maximum, and the similar values of this maximum, for mixtures with acetone and IPA can not be explained considering only production reactions (13-14) and loss ones (15-17). This can be more rigorously demonstrated using the self-consistent kinetic model described in the previous part. In figure 6 are plotted predictions of the model compared to experimental results, for 1 % and 20 % of oxygen; two different kinetic schemes have been used for IPA, either taking into account a temperature dependence for k_{14} (using ethanol parameters) or not. For these computations, all dissociation reactions (1-10) and (18-23) have been disregarded, so that the only possible mechanisms to produce OH are oxidation reactions (13) and (14). It can be seen that the predicted radical density is lower than the measured one for acetone, whatever the oxygen percentage in the mixture; for IPA it depends upon the kinetic scheme used, but for both molecules the time at which the maximum density is reached is much higher for computation results than for measurements. This effect is the more

pronounced for acetone. For IPA the predicted time for $[\text{OH}]_{\text{Max}}$ and the value of this density are very different (higher) than those obtained for acetone, contrary to experimental results.

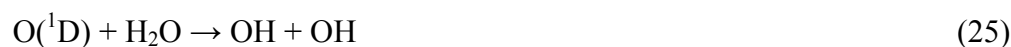
4.3 Effect of dissociation reactions

Predictions of the self-consistent model can be very different from results discussed above if ones take into account dissociation reactions (1-10) and (18-23), added to the previous kinetic schemes. New schemes can be proposed according to possible exit channels for quenching collisions of nitrogen excited states on acetone and IPA. These schemes are resumed in tables 2A (acetone) and 2B (IPA). Results are compared with measurements on figure 7 for 20 % oxygen in the mixture. These computations have been performed without considering a temperature dependence of the oxidation coefficient k_{14} .

It is clear from figure 7 that dissociation processes though collisions with N_2 states play a very important role on the OH density. In particular, contrary to results given on figure 6, the predicted time of the maximum density is closer to the experimental one for case A, i.e. only reactions (18) and (22) together with (21), and for case B, i.e. all reactions (18-20) and reactions (22-23) together with (21). Cases C and D give predictions much far from measurements (values of $[\text{OH}]_{\text{Max}}$ and time for this density to be reached), so that production of only the hydroxyl radical (IPA) or only the methyl group (acetone and IPA) can probably be disregarded. Case A gives the best agreement both for acetone and IPA at 20 % oxygen. However we have checked that for lower oxygen percentage values, the model overestimates $[\text{OH}]_{\text{Max}}$ as it can be seen on figure 8. Lower is the oxygen percentage, higher is the difference between predictions and experimental results. Similar conclusions are obtained in case B. Future works should be devoted to the effect of carbonated by-products kinetics (for example CH_3) in order to check influence of such by-products on the OH density time evolution.

5. Experimental results for wet mixtures

In order to obtain more information about the OH production efficiency in dry mixtures, we have also measured the density of radicals in mixtures containing water vapour (2.3 %). In this case OH is produced during the current pulse by



In figure 9 are compared the OH density time evolution measured for $\text{N}_2/\text{O}_2/\text{VOC}$ mixtures with ones obtained for $\text{N}_2/\text{O}_2/\text{H}_2\text{O}$ and $\text{N}_2/\text{O}_2/\text{H}_2\text{O}/\text{VOC}$ (VOC : acetone or IPA). The oxygen percentage has been fixed to 20 %.

Addition of water vapour to N₂/O₂/VOC mixtures induces an increase of the radical density at short times. However this increase is not very strong, the difference between [OH]_{Max} values measured in dry and in wet mixtures being about 2x10¹⁴ cm⁻³. It emphasises that the role of the VOC molecule in the production of OH is quite important, strengthening that oxidation reactions (13) and (14) do not play the major role in this production. The reactivity of OH with the pollutant molecule and by-products, radicals or molecules, which follow the degradation of the pollutant can be seen if ones compare the decrease of the OH density for N₂/O₂/H₂O and N₂/O₂/H₂O/VOC mixtures. The decrease of the OH density is the slowest for mixtures without VOC. Addition of acetone leads to a faster decrease, but the difference is not very important. Addition of IPA induces a greater effect. This is consistent with known values of rate constants for reactions (15) and (16-17), i.e. (k₁₆+k₁₇)/k₁₅ = 12 in conditions of our experiment. However other processes should also be involved. This will be studied using the self-consistent kinetic model in the future.

6. Conclusions

The production of the hydroxyl radical was studied at a total pressure of 460 mbar in $N_2/O_2/H_2O$ mixtures with addition of 0.5 % of acetone or isopropyl alcohol, using a photo-triggered discharge. The time evolution of the OH density was measured in absolute value by UV-absorption during the afterglow. For dry mixtures, the main parameter was the oxygen percentage, chosen from 1 % up to 20 %. Measurements were compared to predictions of a self-consistent OD discharge and kinetic model. Effect of 2.3 % H_2O added to the mixture was studied experimentally for 20 % of oxygen.

The main conclusions of this study are :

- i/ the production of the hydroxyl radical can not be explained only by reactions of the VOCs with the oxygen atom $O(^3P)$;
- ii/ quenching collisions of the nitrogen excited states on acetone and isopropyl alcohol play an important role in the production of OH;
- iii/ the most probable exit channels for these quenching collisions are, for acetone, productions of H, or of H and CH_3 , together with $O(^3P)$, and for isopropyl alcohol, productions of H, or of the three radicals H, OH, and CH_3 .

As a result of point ii/, the OH maximum density is equal to a few percent of the density of the oxygen atom produced during the discharge, and the N_2 states quenching reactions should be important for the conversion of the pollutant molecules. Acetone and isopropyl alcohol should be more efficiently removed by the hydroxyl radical than by the oxygen atom at low temperature and high initial molecule concentration.

These results are only preliminary ones (in particular point iii/) because we have not taken into account a detailed kinetic scheme for carbonated by-products created either by VOCs dissociation processes or by oxidation reactions. Moreover works have also to be done to determine more precisely rate constants for N_2 states quenching reactions. However, experimental results obtained in wet mixtures confirmed the importance of the VOCs dissociation processes. The self-consistent model will be also developed for these mixtures in the future.

References

- [1] L. Rosocha, and R. Korzekwa, *J. Adv. Oxid. Technol.* **4**, 247 (1999)
- [2] K. Yan, E. van Heesch, A. Pemen, and P. Huijbrechts, *Plasma Chem. Plasma Proc.* **21**, 107 (2001)
- [3] H-H. Kim, *Plasma Process. Polym.* **1**, 91 (2004)
- [4] J. Van Durne, J. Dewulf, C. Leys, and H. Van Langenhove, *Appl. Cat. B* **78**, 324 (2008)
- [5] L. Magne, S. Pasquiers, N. Blin-Simiand, and C. Postel, *J. Phys. D* **40**, 3112 (2007)
- [6] B. Lacour, V. Puech, and S. Pasquiers, *Recent Res. Develop. Appl. Phys.* **6**, 149 (2003)
- [7] M. Rozoy, C. Postel, and V. Puech, *Plasma Sources Sci. Technol.* **8**, 337 (1999)
- [8] F. Fresnet, G. Baravian, L. Magne, S. Pasquiers, C. Postel, V. Puech, and A. Rousseau, *Plasma Sources Sci. Technol.* **11**, 152 (2002)
- [9] J. Jarrige, N. Blin-Simiand, F. Jorand, L. Magne, S. Pasquiers, and C. Postel, in *Proceedings of the XVIIth International Symposium on Plasma Chemistry*, edited by J. Mostahimi, T. Coyle, V. Pershin, and H. Jazy (Toronto, Canada, 2005), p.248-249, and also 6 pages on CD-ROM
- [10] N. Blin-Simiand, F. Jorand, L. Magne, S. Pasquiers, and C. Postel, in *Proceedings of the 5th International Symposium of Non-Thermal Plasma Technology for Pollution Control and Sustainable Development (ISNTPT-5)*, 2006, CD-ROM.
- [11] O. Sarroukh, F. Jorand, C. Postel, L. Magne, and S. Pasquiers, in *Proceedings of the XVIth International Conference on Gas Discharges and their Applications*, edited by Xi'an Jiaotong University (Xi'an, China, 2006), p. 417.
- [12] T. Oda, A. Kumada, K. Tanaka, and S. Masuda, *J. Electrostat.* **35**, 93 (1995)
- [13] V. Zlotopol'skii, and T. Smolenskaya, *High Ener. Chem.* **30**, 188 (1996)
- [14] T. Oda, R. Yamashita, I. Haga, T. Takahashi, and S. Masuda, *IEEE Trans. Indust. Appl.* **32**, 118 (1996)
- [15] Z. Falkenstein, *J. Adv. Oxid. Technol.* **2**, 223 (1997)
- [16] M. Hsiao, B. Penetrante, B. Merritt, G. Vogtlin, and P. Wallman, *J. Adv. Oxid. Technol.* **2**, 306 (1997)
- [17] M. Sobacchi, A. Saveliev, A. Fridman, A. Gutsol, and L. Kennedy, *Plasma Chem. Plasma Proc.* **23**, 347 (2003)
- [18] J. Jarrige, and P. Vervisch, *J. Appl. Phys.* **99**, 113303 (2006)

- [19] M. Malik, and J. Xuan-Zhen, *J. Environ. Sci.* **10**, 276 (1998)
- [20] T. Yamamoto, *J. Haz. Mat. B* **67**, 165 (1999)
- [21] V. Demidiouk, and J. Chae, *IEEE Trans. Plasma Sci.* **33**, 157 (2005)
- [22] C-L. Chang, and T-S. Lin, *Plasma Chem. Plasma Proc.* **25**, 227 (2005)
- [23] F. Holtzer, F. Kpinke, and U. Roland, *Plasma Chem. Plasma Proc.* **25**, 595 (2005)
- [24] Ch. Subrahmanyam, A. Renken, and L. Kiwi-Minsker, *Plasma Chem. Plasma Proc.* **27**, 13 (2007)
- [25] A. Besov, and A. Vorontsov, *Plasma Chem. Plasma Proc.* **27**, 624 (2007)
- [26] H. Brunet, B. Lacour, J. Rocca-Serra, M. Legentil, S. Mizzi, S. Pasquiers, and V. Puech, *J. Appl. Phys.* **68**, 4474 (1990)
- [27] P.Ségur, and M-C.Bordage, *Proceedings of XIXth International Conference on Phenomena in Ionized Gases*, edited by J. Labat, University of Beograd (Beograd, Serbia, 1989), p. 86, and references therein
- [28] J-R. Vacher, F. Jorand, N. Blin-Simiand, and S. Pasquiers, *Int. J. Mass Spect.* **273**, 117 (2008)
- [29] J-R. Vacher, N. Blin-Simiand, F. Jorand, and S. Pasquiers, *Chem. Phys.* **323**, 587 (2006)
- [30] A. Chouki, PhD Thesis, Université Paul Sabatier, France (July 1994)
- [31] W. Mallard, F. Westley, J. Herron, R. Hampson, and D. Frizzell, *NIST Chemical kinetics database version 2Q98* (1998)
- [32] I. Kossyi, A. Kostinsky, A. Matveyev, and V. Silakov, *Plasma Sources Sci. Technol.* **1**, 207 (1992)
- [33] R. Atkinson, D. Baulch, R. Cox, R.Hampson, J. Kerr, M. Rossi, and J. Troe, *J. Phys. Chem. Ref. Data* **28**, 191 (1999) ; and references therein
- [34] W. Clark, and D. Setser, *J. Phys. Chem.* **84**, 2225 (1980).
- [35] O. Sarroukh, F. Jorand, L. Magne, C. Postel, S. Pasquiers in *Proceedings of the 5th International Symposium of Non-Thermal Plasma Technology for Pollution Control and Sustainable Development (ISNTPT-5)*, 2006, CD-ROM.

Table 1

List of heavy species reactions with their rate constants. Reaction coefficients are given by the Arrhénius function :

$$K = K_0 T_g^A \exp(B/T_g)$$

where T_g is the gas mixture temperature (in K).

(*) : temperature dependence corresponding to ethanol.

		k_0	A	B
13	$O(^3P) + CH_3COCH_3 \rightarrow OH + CH_3COCH_2$	1.66 (-11)	0	-3000
14	$O(^3P) + CH_3CH(OH)CH_3 \rightarrow OH + \text{products}$	6.64 (-14)	0	0
14*	$O(^3P) + CH_3CH(OH)CH_3 \rightarrow OH + \text{products}$	1.23 (-18)	2.46	-930
15	$OH + CH_3COCH_3 \rightarrow H_2O + CH_3COCH_2$	2.8 (-12)	0	-760
16	$OH + CH_3CH(OH)CH_3 \rightarrow H_2O + CH_3C(OH)CH_3$	2.44 (-12)	0	200
17	$OH + CH_3CH(OH)CH_3 \rightarrow H_2O + CH_3CH(OH)CH_2$	0.16 (-12)	0	200
<i>Case A</i>				
18	$N_2(A^3\Sigma_u^+) + CH_3CH(OH)CH_3 \rightarrow CH_3CH(OH)CH_2 + H$	1.0 (-10)	0	0
	$N_2(a') + CH_3CH(OH)CH_3 \rightarrow CH_3CH(OH)CH_2 + H$	1.0 (-10)	0	0
22	$N_2(A^3\Sigma_u^+) + CH_3COCH_3 \rightarrow CH_3COCH_2 + H$	1.0 (-10)	0	0
21	$N_2(a') + CH_3COCH_3 \rightarrow CH_3CCH_3 + O(^3P)$	1.0 (-10)	0	0
<i>Case B</i>				
18	$N_2(A^3\Sigma_u^+) + CH_3CH(OH)CH_3 \rightarrow CH_3CH(OH)CH_2 + H$	0.33 (-10)	0	0
	$N_2(a') + CH_3CH(OH)CH_3 \rightarrow CH_3CH(OH)CH_2 + H$	0.33 (-10)	0	0
19	$N_2(A^3\Sigma_u^+) + CH_3CH(OH)CH_3 \rightarrow CH_3CH(OH) + CH_3$	0.33 (-10)	0	0
	$N_2(a') + CH_3CH(OH)CH_3 \rightarrow CH_3CH(OH) + CH_3$	0.33 (-10)	0	0
20	$N_2(A^3\Sigma_u^+) + CH_3CH(OH)CH_3 \rightarrow CH_3CHCH_3 + OH$	0.33 (-10)	0	0
	$N_2(a') + CH_3CH(OH)CH_3 \rightarrow CH_3CHCH_3 + OH$	0.33 (-10)	0	0
22	$N_2(A^3\Sigma_u^+) + CH_3COCH_3 \rightarrow CH_3COCH_2 + H$	0.5 (-10)	0	0
23	$N_2(A^3\Sigma_u^+) + CH_3COCH_3 \rightarrow CH_3CO + CH_3$	0.5 (-10)	0	0
21	$N_2(a') + CH_3COCH_3 \rightarrow CH_3CCH_3 + O(^3P)$	1.0 (-10)	0	0
<i>Case C</i>				
19	$N_2(A^3\Sigma_u^+) + CH_3CH(OH)CH_3 \rightarrow CH_3CH(OH) + CH_3$	1.0 (-10)	0	0
	$N_2(a') + CH_3CH(OH)CH_3 \rightarrow CH_3CH(OH) + CH_3$	1.0 (-10)	0	0
23	$N_2(A^3\Sigma_u^+) + CH_3COCH_3 \rightarrow CH_3CO + CH_3$	1.0 (-10)	0	0
21	$N_2(a') + CH_3COCH_3 \rightarrow CH_3CCH_3 + O(^3P)$	1.0 (-10)	0	0
<i>Case D</i>				
20	$N_2(A^3\Sigma_u^+) + CH_3CH(OH)CH_3 \rightarrow CH_3CHCH_3 + OH$	1.0 (-10)	0	0
	$N_2(a') + CH_3CH(OH)CH_3 \rightarrow CH_3CHCH_3 + OH$	1.0 (-10)	0	0

Table 2A

Proposed exit channels for quenching collisions of nitrogen excited states with acetone.

	$N_2(A^3\Sigma_u^+)$	$N_2(a')$
Case A	H only	$O(^3P)$
Case B	H (50 %) and CH_3 (50 %)	$O(^3P)$
Case C	CH_3 only	$O(^3P)$

Table 2B

Proposed exit channels for quenching collisions of nitrogen excited states with iso-propyl alcohol.

	$N_2(A^3\Sigma_u^+)$ and $N_2(a')$
Case A	H only
Case B	H (33 %) and OH (33 %) and CH_3 (33 %)
Case C	CH_3 only
Case D	OH only

Figure captions

Figure 1 – Experimental set-up.

Figure 2 – OH absorption spectra in the N₂/O₂/ iso-propyl alcohol mixture with 10 % O₂ and 0.5 % iso-propyl alcohol : a) 2 μs and b) 15 μs after the discharge.

Figure 3 – Predicted densities for atoms and excited states of (a) nitrogen and (b) oxygen and ozone in the N₂/O₂ mixture with 20 % oxygen. Molecular levels clustered in effective states are circled.

Figure 4 – Hydroxyl radical density as function of time for N₂/O₂ mixtures with addition of 0.5 % of : a) acetone and b) iso-propyl alcohol. Percentage values of oxygen are given on diagrams.

Figure 5 – Maximum OH density as function the oxygen percentage in N₂/O₂ mixtures with addition of 0.5 % of acetone or iso-propyl alcohol. [O]_{Max} is the maximum oxygen density predicted by the self-consistent 0D discharge and kinetic model.

Figure 6 – Measured and predicted time evolutions of the OH density for mixtures with : a/ 1 % oxygen, b/ : 20 % oxygen. Predictions are for very simplified kinetic schemes taking into account only oxidation reactions (13-17) (see text). For iso-propyl alcohol, the dotted lines correspond to a kinetic scheme including a temperature dependence for the reaction of O(³P) with the molecule (reaction 14). Same symbols and lines for diagrams a/ and b/.

Figure 7 – Measured and predicted time evolutions of the OH density for mixtures with 20 % oxygen : a/ acetone, b/ iso-propyl alcohol. Exit channels for quenching collisions of nitrogen excited states (A, B, C, D) are given in tables 2A (acetone) and 2B (iso-propyl alcohol).

Figure 8 – Predicted maximum OH density (lines) in case A (see table 2A and 2B) compared to experimental results (symbols, triangles : acetone, squares : iso-propyl alcohol).

Figure 9 – Hydroxyl radical density as function of time for various dry and wet mixtures : a) acetone and b) iso-propyl alcohol.

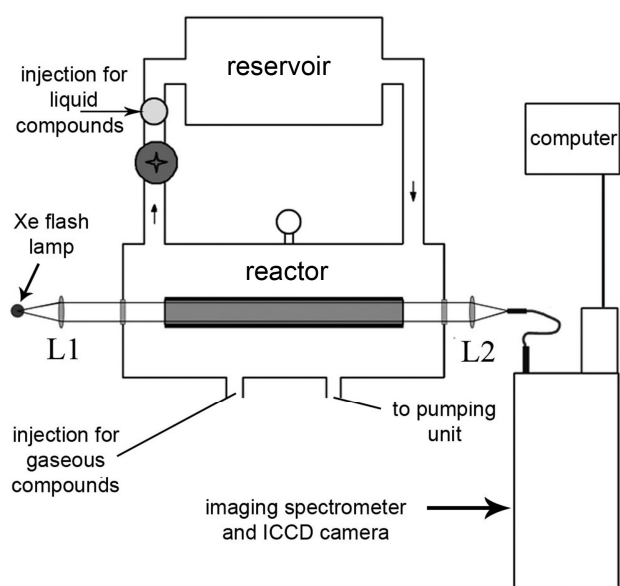


Figure 1 – Experimental set-up.

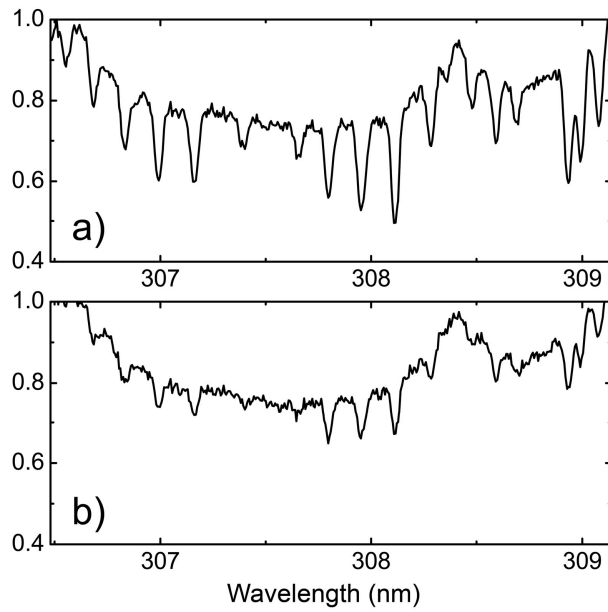


Figure 2 – OH absorption spectra in the N_2/O_2 / iso-propyl alcohol mixture with 10 % O_2 and 0.5 % iso-propyl alcohol : a) 2 μs and b) 15 μs after the discharge.

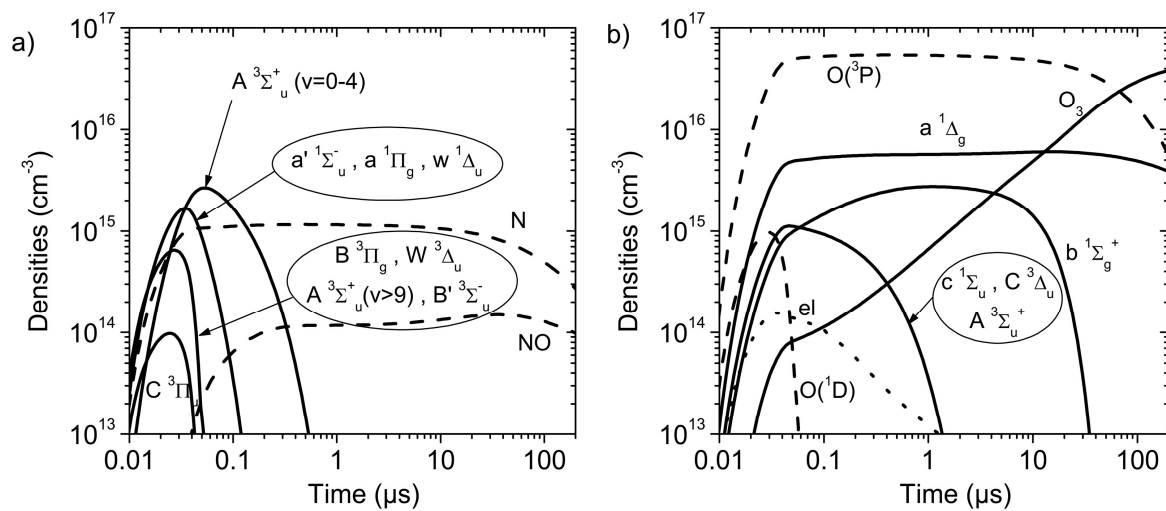


Figure 3 – Predicted densities for atoms and excited states of (a) nitrogen and (b) oxygen and ozone in the N₂/O₂ mixture with 20 % oxygen. Molecular levels clustered in effective states are circled.

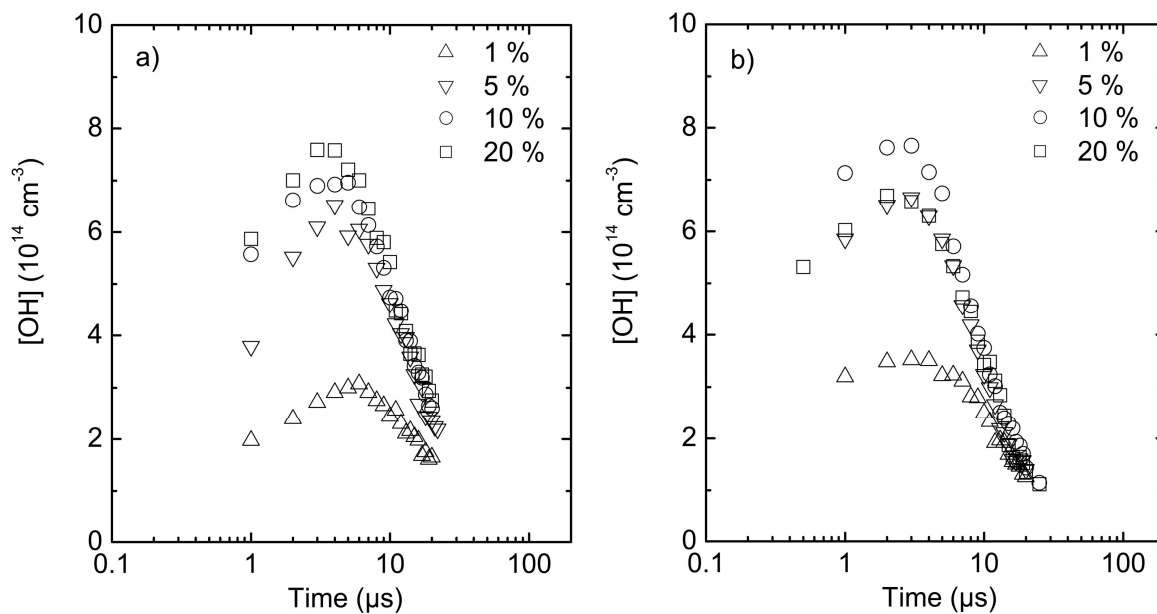


Figure 4 – Hydroxyl radical density as function of time for N_2/O_2 mixtures with addition of 0.5 % of : a) acetone and b) iso-propyl alcohol. Percentage values of oxygen are given on diagrams.

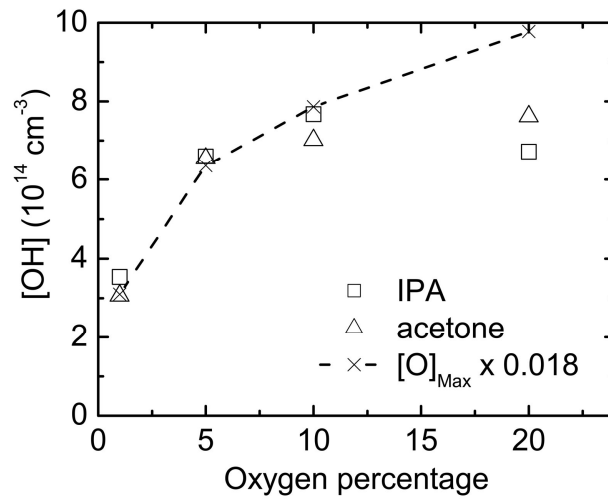


Figure 5 – Maximum OH density as function the oxygen percentage in N₂/O₂ mixtures with addition of 0.5 % of acetone or iso-propyl alcohol. [O]_{Max} is the maximum oxygen density predicted by the self-consistent 0D discharge and kinetic model.

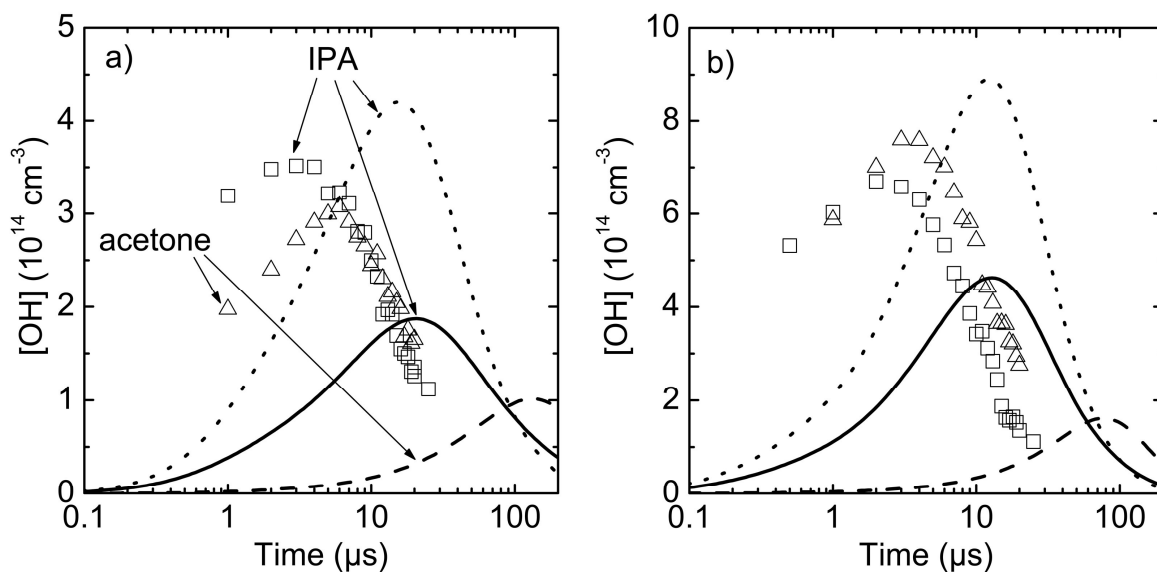


Figure 6 – Measured and predicted time evolutions of the OH density for mixtures with : a/ 1 % oxygen, b/ : 20 % oxygen. Predictions are for very simplified kinetic schemes taking into account only oxidation reactions (13-17) (see text). For iso-propyl alcohol, the dotted lines correspond to a kinetic scheme including a temperature dependence for the reaction of $\text{O}(^3\text{P})$ with the molecule (reaction 14). Same symbols and lines for diagrams a/ and b/.

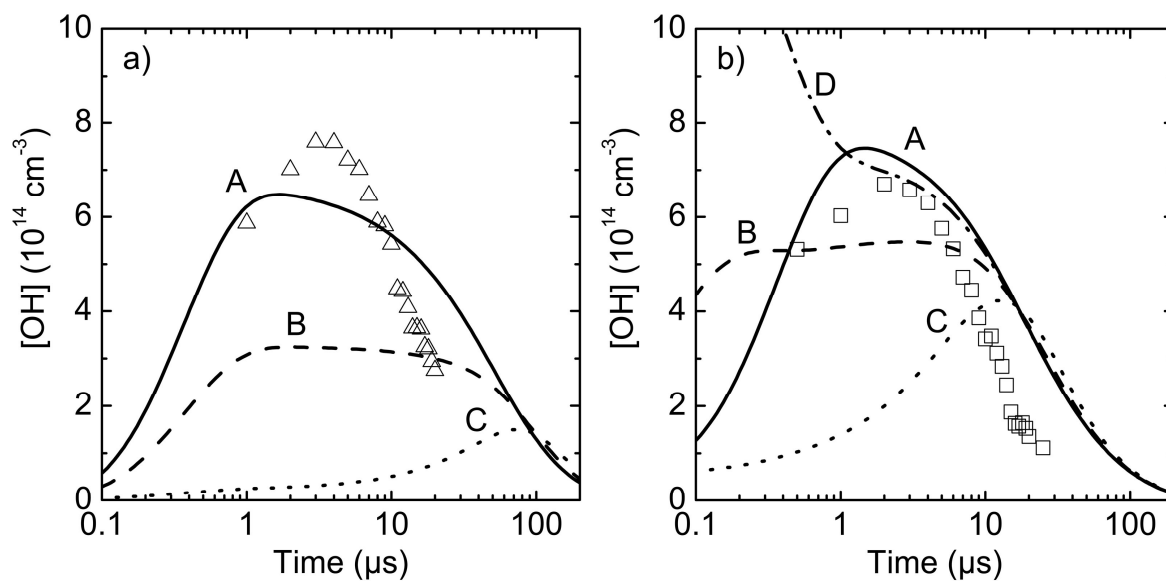


Figure 7 – Measured and predicted time evolutions of the OH density for mixtures with 20 % oxygen : a/ acetone, b/ iso-propyl alcohol. Exit channels for quenching collisions of nitrogen excited states (A, B, C, D) are given in tables 2A (acetone) and 2B (iso-propyl alcohol).

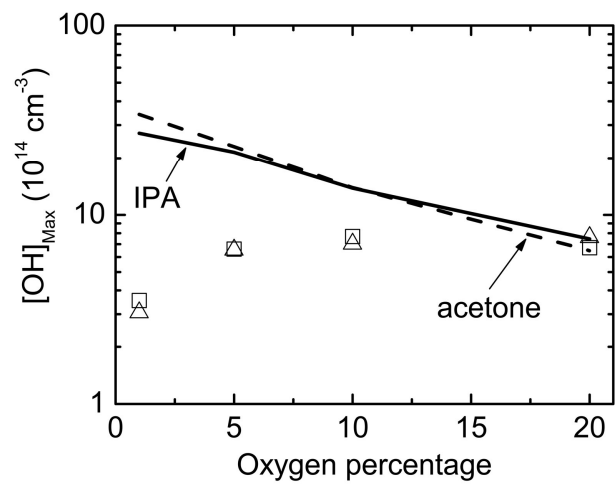


Figure 8 – Predicted maximum OH density (lines) in case A (see table 2A and 2B) compared to experimental results (symbols, triangles : acetone, squares : iso-propyl alcohol).

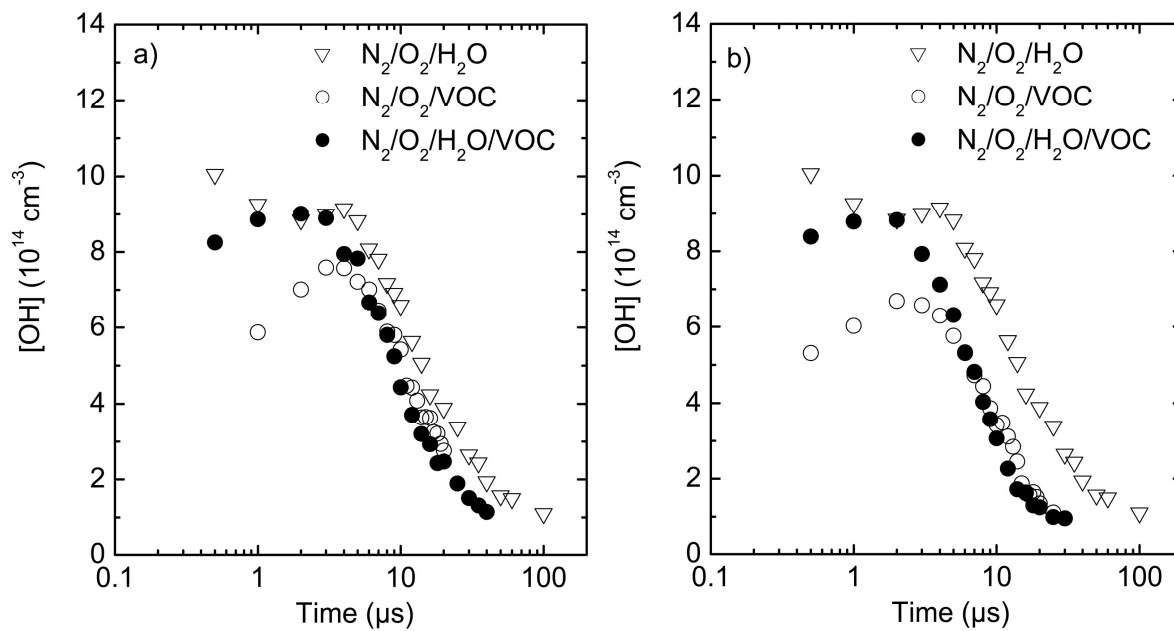


Figure 9 – Hydroxyl radical density as function of time for various dry and wet mixtures : a) acetone and b) iso-propyl alcohol.